Applied Organometallic Chemistry

Received: 2 February 2010 Revised: 25 April 2010 Accepted: 26 April 2010 Published online in Wiley Online Library: 7 July 2010

(wileyonlinelibrary.com) DOI 10.1002/aoc.1682

Photoluminescent and oxygen sensing properties of core–shell nanospheres based on a covalently grafted ruthenium(II) complex

Shuli Wang[a], Bin Li[a]*, Liming Zhang[b], Lina Liu[b] and Yinghui Wang[b]

SiO_2 nanospheres coated with silica chemically doped with a ruthenium complex $[Ru(Bphen)_2Phen–Si]Cl_2$ (denoted as Ru, there Bphen = 4,7-diphenyl-1,10-phenanthrolin, Phen–Si = modified 1,10-phenathroline) were prepared using a simple solution-based method. Field-emission scanning electron microscopy (FE-SEM) showed that the pure SiO_2 nanospheres with a mean diameter of ∼185 nm were successfully coated with Ru complex–chemically doped SiO_2 shell with a thickness of ∼45 nm. The obtained core-shell nanosphere materials exhibited bright red triplet metal-to-ligand charge transfer (^{3}MLCT) emission, and their photoluminescent intensity was sensitive to oxygen concentration. These properties make them promising candidates for biomarkers and optical oxygen sensors, which can measure the O_2 concentration in biological fluids. Copyright © 2010 John Wiley & Sons, Ltd.

Keywords: composites; chemical synthesis; infrared spectroscopy; luminescence

Introduction

Functional nanostructured and nanocomposite materials have received much attention.[1–6] The determination of oxygen concentration is critical for the existence of life. Recent interest in methods for measuring O_2 has been mainly focused on optical sensors due to their advantages over conventional amperometric electrodes in that they are faster, do not consume oxygen and are not easily poisoned.[7–10] Many luminescent dyes have been tested as oxygen sensing probes. Among them, ruthenium(II) complexes are one of the most widely used due to their highly emissive metal-to-ligand charge transfer (MLCT) state, long fluorescence lifetime, large Stokes shift, high photochemical stability, high sensitivity to oxygen and strong visible absorption in the blue-green region. However, they have inherent limitations, such as triplet–triplet self-quenching. To avoid this, it is necessary to find matrices for Ru(II) complexes.[11,12] Among these matrices, considerable efforts have been paid to silica nanospheres since silica is nontoxic and highly biocompatible.[13–15] The encapsulation of fluorescent dyes in SiO_2 nanospheres often increases their photostability and emission quantum yield due to the isolation from possible quenchers. Besides, the surface of SiO_2 contains free silanol groups, which can react with appropriate drug functional groups, and are easily functionalized and modified with amines, thiols and carboxyl groups, facilitating the linking of biomolecules such as biotin and avidin.[16]

In this paper, we prepared Ru(II) complex covalently immobilized onto silica nanospheres surface layer (SiO_2@Ru) using the Stöber method, which is simple and carried out in an ethanol–water mixture, completely avoiding the use of potentially toxic organic solvents and surfactants.[17] Furthermore, slight modification of the ammonia and water contents in the reaction mixture results in shells with different thicknesses.[18] The Stern–Volmer plots of SiO_2@Ru show good linearity at concentrations of oxygen ranging from 0 to 60%, which endow this kind of nanospheres with the potential to measure the O_2 concentration in biological fluids.

Experimental Section

Materials and Synthesis

Anhydrous $RuCl_3$ (99.99%) was obtained from Acros Organics (Geel, Belgium). 3-(Triethoxysilyl)propyl isocyanate (TEPIC) and the 5% Pd–C catalyst were purchased from Aldrich (Milwaukee, WI, USA). The complex $Ru(Bphen)_2Cl_2 \cdot 2H_2O$ was synthesized and purified as described in the literature.[19] $NH_3 \cdot H_2O$, tetraethoxysilane (TEOS), hexane, chloroform and ethanol were obtained from Beijing Chemical Company. The water used in our present work was deionized.

The synthesis of the nanocomposite materials is shown in Fig. 1. SiO_2 nanospheres were first prepared following the well-known Stöber method. Then TEOS together with Ru complex hydrolyzed on the surface of SiO_2 to form nanospheres with a covalently linked Ru(II) complex.

Preparation of Phen–Si

The Phen–Si was prepared using 5-amino-1,10-phenanthroline (Phen–NH_2) and TEPIC as the starting materials.[20] The synthesis of Phen–NH_2 was performed by nitration of 1,10-phenanthroline in a mixture of concentrated sulfuric acid and fuming nitric acid,

* *Correspondence to: Bin Li, Key Laboratory of Polyoxometalate Science of Ministry of Education, Faculty of Chemistry, Northeast Normal University, Renmin Street No. 5268, Changchun, 130024, People's Republic of China. E-mail: lib020@yahoo.cn*

a *Key Laboratory of Polyoxometalate Science of Ministry of Education, Faculty of Chemistry, Northeast Normal University, Renmin Street No. 5268, Changchun, 130024, People's Republic of China*

b *Key Laboratory of Excited State Processes, Changchun Institute of Optics, Fine Mechanics and Physics, Chinese Academy of Sciences, Changchun, 130033, People's Republic of China*

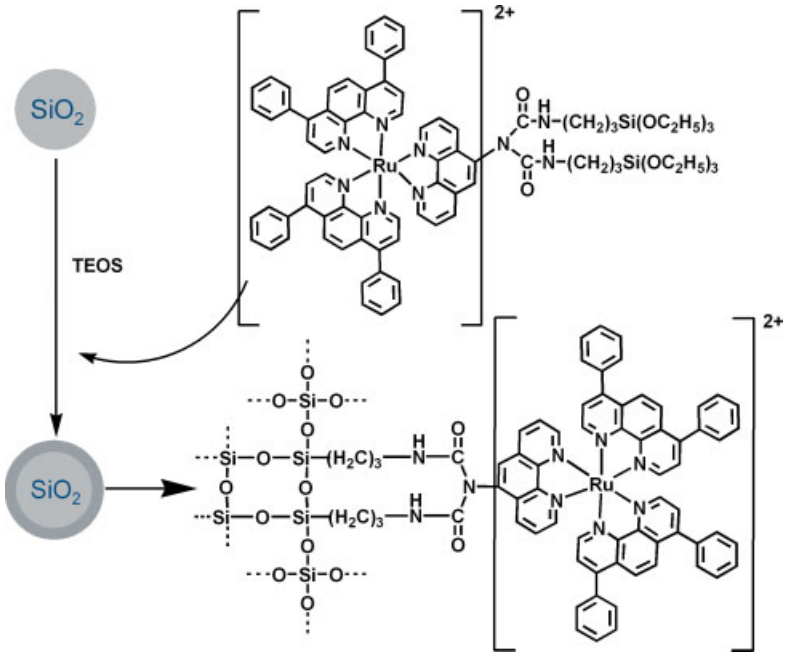

Figure 1. Schematic diagram of the synthetic procedure.

followed by reduction of the nitro derivative with hydrazine over a 5% Pd–C catalyst. Their identities were confirmed by ^{1}H NMR and elemental analysis. ^{1}H NM (300 MHz, $CDCl_3$) δ (ppm): 9.23 (m, 2 H), 8.24 (m, 2 H), 7.86 (s, 1H), 7.67 (m, 2 H), 7.16 (s,2 H), 3.69 (quartet, 12H), 3.21 (m, 4H), 1.60 (m, 4H), 1.13(t, 18H), 0.52(m,4H). Elemental analysis: calculated for $C_{32}H_{51}N_5O_8Si_2$: C, 55.70; H, 7.45; N, 10.15%. Found C, 55.89; H, 7.34; N, 10.20%.

Preparation of [Ru(Bphen)$_2$Phen–Si]Cl$_2$

The complex Ru was synthesized by modifying a reported procedure.[21] A mixture of $Ru(Bphen)_2Cl_2$ and Phen–Si in anhydrous ethanol was refluxed for 8 h in a nitrogen atmosphere to give a transparent deep red solution, indicating that the complexation reaction between Phen–Si and $Ru(Bphen)_2Cl_2$ had finished. The molar ratio of Phen–Si to $Ru(Bphen)_2Cl_2$ was 1.02 : 1. Finally the ethanol was rotary evaporated off and the residue was recrystallized by vapor diffusion of diethyl ether into its ethanol solution and dried in a vacuum.

Synthesis of luminescent nanocomposite materials

The synthesis of highly monodisperse SiO_2 spheres was carried out following the well-known Stöber method, that is, TEOS hydrolyzed in an ethanol solution containing water and ammonia.[22] The nanospheres were dispersed in absolute ethanol. In a typical synthesis, a solution of 160 ml absolute ethanol and 15 ml water was added into the above solution, then 0.20 ml TEOS and sample Ru complex (200 mg g^{-1} SiO_2) were added to the solution. The solution was put into an ultrasonic bath for 2 h at room temperature. Finally the product was collected, washed and dried. The obtained luminescent nanocomposite materials were labeled as sample SiO_2@Ru.

Measurements

Field-emission scanning electron microscopy (FE-SEM) images were measured on a Hitachi S-4800 microscope. The IR absorption spectra were measured in the range 400–4000 cm^{-1} using an FT-IR spectrophotometer (model Bruker Vertex 70 FT-IR) with a resolution of $\pm$4 cm^{-1} using the KBr pellet technique. The powder samples were dispersed in absolute ethanol by ultrasonic to form a uniform suspension for the measurements of the UV–vis absorption spectra, which were performed on a UV-3101PC UV–vis–NIR scanning spectrophotometer (Shimadzu) at room temperature. The photoluminescent emission spectra were recorded at room temperature with a Hitachi F-4500 spectrophotometer equipped with a continuous 150 W Xe-arc lamp. The fluorescence was measured by a UV-Lab Raman Infinity (Jobin Yvon) with a resolution of 2 cm^{-1}. In the fluorescence dynamics measurements, a 355 nm light generated from the Nd^{3+} – YAG laser combined with a fourth-harmonic generator was used as the pump, with a repetition frequency of 10 Hz and pulse duration of 10 ns. A two-channel Tektronix TDS-3052 oscilloscope was used to record the fluorescence decay curves. The oxygen-sensing properties of the obtained samples were discussed on the basis of the photoluminescence intensity quenching instead of the excited-state lifetime because it is hard to obtain the precise excited-stated lifetime values under quenched conditions. The oxygen-sensing properties based on luminescence intensity quenching of sample Ru complex were characterized using the same Hitachi F-4500 fluorescence spectrophotometer. For measurement of the Stern–Volmer plot, oxygen and nitrogen were mixed at different concentrations via gas flow controllers and passed directly to the sealed gas chamber. We typically allowed 1 min between changes in the N_2/O_2 concentration to ensure that a new equilibrium point had been established. The time-scanning curves were obtained using the same method.

Results and Discussion

Structure and Morphology

Figure 2 shows the SEM images of the SiO_2 and SiO_2@Ru nanospheres. The SiO_2 nanospheres with a mean diameter of

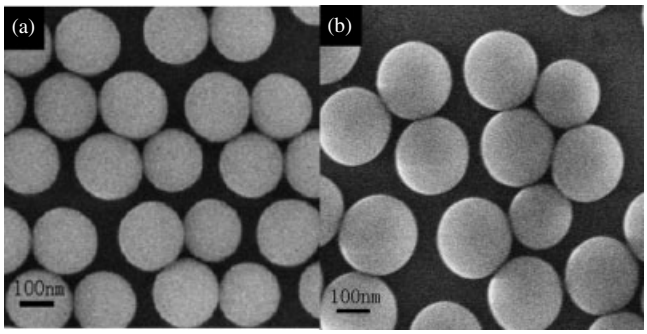

Figure 2. SEM images of SiO_2 nanospheres (a) and sample SiO_2@Ru (b).

Figure 3. The fluorescence image of sample SiO_2@Ru in solid state (magnified four times).

~185 nm were uniform and monodisperse, making possible the next coating procedure. The obtained nanospheres SiO_2@Ru had a mean diameter of ~230 nm, indicating that SiO_2 nanospheres were successfully coated with Ru complex complex–chemically doped SiO_2 shell with a thickness of ~45 nm. The thickness of shell could be altered by changing the TEOS concentration. The fluorescence image of sample SiO_2@Ru shows bright red emission of Ru(II) complex arising from the MLCT excited state (as shown in Fig. 3).

FT-IR Spectra

Figure 4 shows that complex Ru has been covalently grafted to the silica nanoparticals using the double-role Phen–Si compound, as a second ligand for $Ru(Bphen)_2Cl_2$. In the IR spectrum of Phen–Si, the peaks located at 1653 and 1541 cm^{-1} correspond to the –CONH– group. The absorption peak at 1091 cm^{-1} (ν_{as}, Si–O–Si) in sample SiO_2@Ru substantiates the formation of a SiO_2 framework.[23,24] In Fig. 4b, the peaks located at 1538, 1647 (the vibrations of –CONH–) and 1693 cm^{-1} (the vibration of –C═O–) in sample SiO_2@Ru is sufficient to prove that the Ru complex was successfully covalently bonded onto SiO_2 networks. In addition, the peaks at 1538, 1647 and 1693 cm^{-1} in sample SiO_2@Ru showed obvious red-shifts compared with 1541, 1653 and 1710 cm^{-1} for free Phen–Si. The complexation between $Ru(Bphen)_2Cl_2$ and the

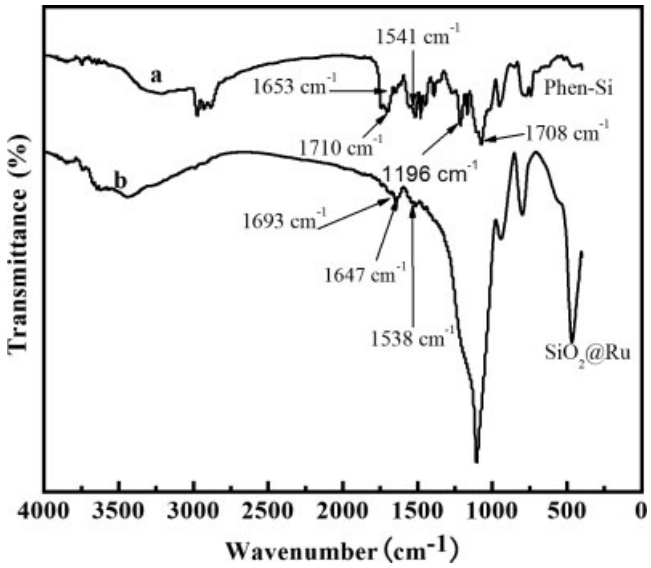

Figure 4. FT-IR spectra for Phen–Si (a) and SiO_2@Ru nanospheres (b).

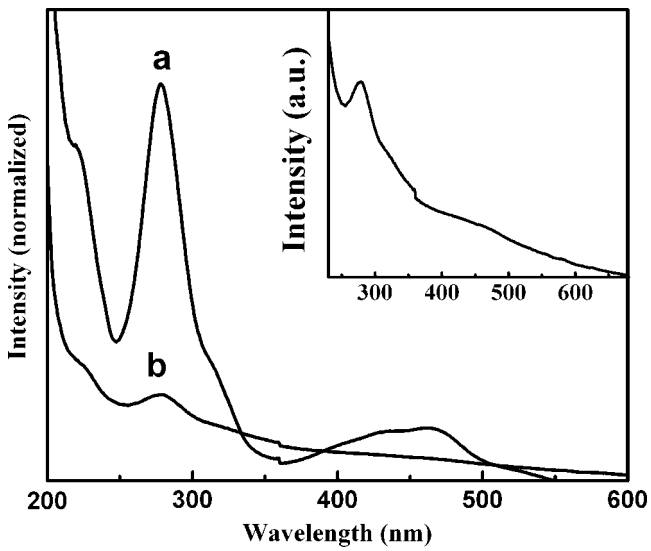

Figure 5. UV–vis absorption spectra for SiO_2@Ru (a) and Ru complex (b) in ethanol. Inset: amplified UV–vis absorption spectra of sample Ru complex in ethanol.

Phen–Si ligand leads to a decrease in their vibration frequencies, which is responsible for the red-shift of the spectra.

UV–vis Absorption Spectra

Figure 5 shows the UV–vis absorption spectra of samples SiO_2@Ru in solid state and pure Ru complex dissolved in ethanol. It can be seen that the pure Ru(II) complex shows two absorption bands centered at 278 and 458 nm. The band at higher energy can be attributed to the ligand-centered ($\pi \rightarrow \pi^*$) transition of Phen and the low energy absorption band is assigned to the singlet MLCT $t_{2g}(Ru) \rightarrow \pi^*$ (L) transition.[25] These two absorption bands were also found in the absorption spectrum of sample SiO_2@ Ru. This provided further evidence that Ru complex had been successfully grafted onto the surface layer of the SiO_2 shell.

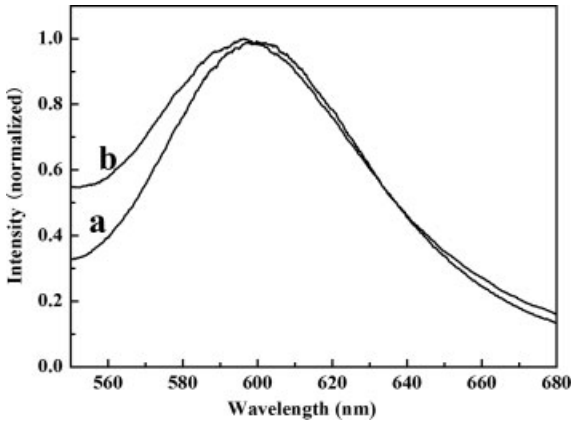

Figure 6. Room temperature emission spectra recorded for SiO_2@Ru nanospheres (a) and Ru(II) complex in water (b) excited at 465 nm.

Photoluminescence

The emission spectra of samples SiO_2@Ru in the solid state and Ru complex in water are shown in Fig. 6. The broad emission band centered at 596 nm for sample Ru complex can be attributed to the transition from the triplet MLCT excited state (^{3}MLCT) to the ground state.[26] The emission maximum in sample SiO_2@Ru was also almost at this position. No emission at 596 nm was observed from the suspension after sample SiO_2@ Ru had been removed by centrifugation, indicating that all the Ru(II) complex was successfully doped into the SiO_2 shell.

Fluorescence Lifetime

The fluorescence decay curves of samples SiO_2@Ru in solid state and Ru complex in ethanol were measured at room temperature at ambient atmosphere. The fluorescence decay curve in sample Ru complex could be fitted to a single-exponential decay curve expressed by

$$I(t) = \alpha \exp(-t/\tau) \quad (1)$$

where $I(t)$ is the fluorescence intensity at time t, τ the decay time and α the pre-exponential factor. However, the fluorescence decay data in sample SiO_2@Ru could be fitted very well to biexponential decay curve expressed by

$$I(t) = a_1 exp(-t/\tau_1) + a_2 exp(-t/\tau_2) \quad (2)$$

where the subscripts 1 and 2 denote the assigned lifetime components and a_i denotes the pre-exponential factors. The weighted mean lifetime τ_m can be calculated by using the following equation:[27]

$$\langle \tau_m \rangle = \sum_{i=1}^{2} \alpha_i \tau_i / \sum_{i=1}^{2} \alpha_i \quad (3)$$

The results of the lifetime measurements are summarized in Table 1, showing that the weighted mean lifetime in sample Ru complex dissolved in ethanol became shorter than that in solid sample of SiO_2@Ru. The lifetime can be written as:

$$\tau = \frac{1}{W_r + W_{nr}} \quad (4)$$

Table 1. Time-resolved intensity decay constants for various samples

Sample	a_1	τ_1 (μS)	a_2	τ_2 (μS)	τ (μS)	r^2
Ru complex	0.162	0.186				0.9973
SiO_2@Ru	0.066	0.150	0.033	1.079	0.459	0.9973

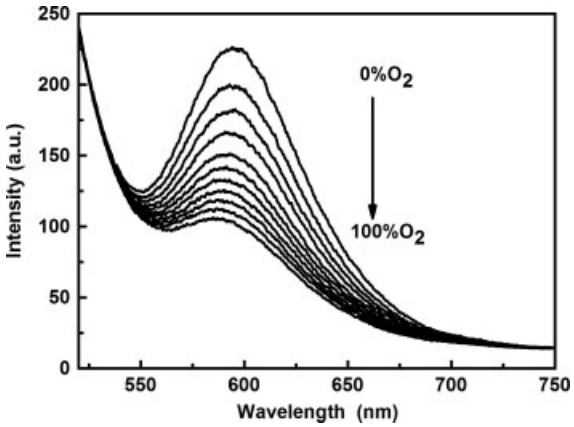

Figure 7. Emission spectra of sample SiO_2@Ru under different oxygen concentrations.

where W_r and W_{nr} are the total radiative transition rate and the nonradiative rate, respectively. When sample Ru complex was dissolved in ethanol, the high-frequency (O–H) modes around 3400 cm^{-1} could take the role of energy acceptors in the nonradiative decay of MLCT excited states.[28,29] The increase of lifetime in sample SiO_2@ Ru can be attributed to the decrease in the υ(O–H) modes, which decreased the nonradiative rate.

Oxygen-sensing Properties

The luminescence of most Ru(II) complexes could be quenched effectively by molecular oxygen. The room temperature emission spectra, which were recorded for sample SiO_2@Ru under different concentrations of oxygen, are presented in Fig. 7; the concentration of oxygen was controlled from 0 to 100%. The position and shape at 596 nm MLCT emission from Ru complex was constant under different oxygen concentrations. However, the relative intensity decreased markedly with increasing the oxygen concentration. The relative luminescent intensities of the Ru complex decreased by 53.2%.

Optical sensors based on the luminescence quenching intensity were examined by Stern–Volmer analysis. In homogeneous media with a single-exponential decay, the intensity form of the Stern–Volmer equation with dynamic quenching was as follows:[30]

$$I_0/I = \tau_0/\tau = 1 + K_{SV} pO_2 = 1 + k\tau_0 pO_2 \quad (5)$$

where I is the fluorescence intensity of the luminophore, the subscript 0 denotes the absence of oxygen, K_{SV} is the Stern–Volmer constant and [O_2] is the oxygen concentration. A plot of I_0/I will be linear with a slope equal to K_{SV}, and an intercept of unity. However, it is more frequent that the distribution of luminescent species in the solid matrix is heterogeneous on a microscopic scale. In this case, the linear Stern–Volmer quenching curves in

Table 2. Intensity-based Stern–Volmer oxygen quenching fitting parameters for SiO_2@Ru

		Stern–Volmer[a]		Demas[b]			
Sample	I_0/I_{100}	$K_{SV1}([O_2]^{-1})$	r^2	$K_{SV1}([O_2]^{-1})$	$K_{SV2}([O_2]^{-1})$	f_{01}	r^2
SiO_2@Ru	2.13	0.01052	0.97053	0.01056	0.00008	0.9923	0.99529

[a] Terms are from equation (5).
[b] Terms are from equation (6): $f_{01} + f_{02} = 1$.

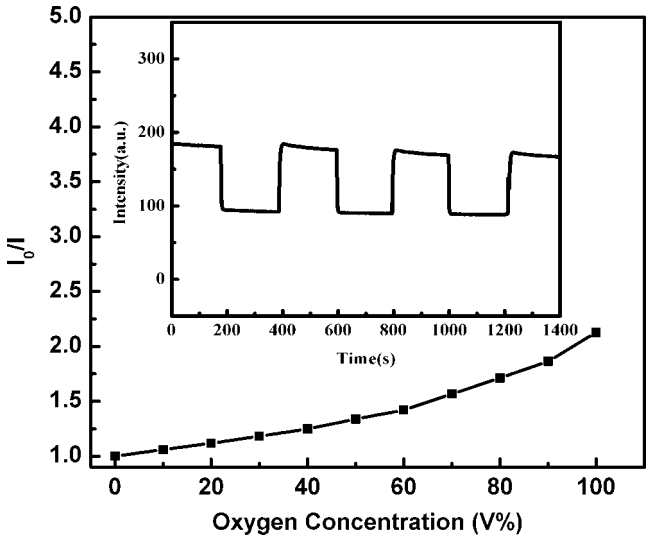

Figure 8. The Stern–Volmer plots for sample SiO_2@Ru nanospheres. Inset: the dynamic response of sample SiO_2@Ru nanospheres.

equation (5) should be recast as follows:[31]

$$I_0/I = 1/[f_{01}/(1 + K_{SV1}pO_2) + f_{02}/(1 + K_{SV2}pO_2)] \quad (6)$$

where f_{0i} is the steady-state fraction of light emitted from the i site and K_{svi} is its Stern–Volmer constant. Equation (6) is the familiar Demas 'two-site' model that has proved to have an excellent ability to describe the nonlinear Stern–Volmer quenching curves.

Figure 8 presents the Stern–Volmer plot for sample SiO_2@Ru. The intensity-based Stern–Volmer oxygen-quenching fitting parameters are also tabulated in Table 2. As shown in Fig. 8, sample SiO_2@Ru shows a good linearity at concentrations of oxygen ranging from 0 to 60%. A linear Stern–Volmer plot is very important for an oxygen sensor because it is easy to calibrate and does not require a multipoint calibration strategy when used for practical applications. The latter part of plot deviates from linearity, which is attributed to a distribution of slightly different quenching environments for the luminophore. The inset of Fig. 8 shows the typical dynamic response of sample SiO_2@Ru upon repeated exposure to nitrogen/oxygen cycles in the gas phase. The emission intensity transformed quickly when the sample was exposed to different gas phases. However, the luminescence intensity showed a small photobleaching effect under light irradiation.

Conclusion

Optical nanospheres containing covalently bonded Ru(II) complex in a silicate network were prepared. They exhibited bright red light. The dye leaching shortcoming was overcome since these luminescence molecules were covalently grafted to the Si–O network using the Si–C bonds. Their phtoluminescent intensity was sensitive to oxygen concentration. A good linearity between the fluorescence intensity of the SiO_2@ Ru complex and the concentration of O_2 over a range of 0–60% was constructed. These properties make them candidates for monitoring the dissolved oxygen in liquid phase, especially for use in biological fluids.

Acknowledgments

The authors gratefully acknowledge the financial support of the One Hundred Talents Project from Chinese Academy of Sciences, the National Natural Science Foundations of China (grant no. 50872130)

References

[1] S. M Liu, Y ang, S Sato, K Kimura, *Chem. Mater.* **2006**, *18*, 637.
[2] S. H Hu, T. Y Liu, H.Y Huang, D. M Liu, S.Y Chen, *Langmuir* **2008**, *24*, 239.
[3] S. C McBain, H. H. P Yiu, A. E Haj, J Dobson, *J. Mater. Chem.* **2007**, *17*, 2561.
[4] L. Y Wang, Y. D Li, *Nano Lett.* **2006**, *6*, 1645.
[5] M. J Li, Z. F Chen, V. W. W Yam, Y. B Zu, *Acs. Nano* **2008**, *2*, 905.
[6] L Levy, Y Sahoo, K. S Kim, E. J Bergey, P. N Prasad, *Chem. Mater.* **2002**, *14*, 371.
[7] M. L Hitchman, *Measurement of Dissolved Oxygen*. Wiley: New York, **1978**.
[8] Z Rosenzweig, R Kopelman, *Anal. Chem.* **1995**, *67*, 2650.
[9] C McDonagh, B. D MacCraith, A. K McEvoy, *Anal. Chem.* **1998**, *70*, 45.
[10] H Xu, J. W Aylott, R Kopelman, T. J Miller, M. A Philbert, *Anal. Chem.* **2001**, *73*, 4124.
[11] Q. C Liu, B Li, J Gong, Y. L Sun, W. L Li, *J. Alloy Compd.* **2008**, *466*, 314.
[12] H. R Zhang, B Li, B. L Lei, W. L Li, S. Z Lu, *Sens. Actuators, B* **2007**, *123*, 508.
[13] S Moudgil, J. Y Ying, *Adv. Mater.* **2007**, *19*, 3130.
[14] D. K Yi, S. S Lee, G. C Papaefthymiou, J. Y Ying, *Chem. Mater.* **2006**, *18*, 614.
[15] H Xu, L. L Cui, N. H Tong, H. C Gu, *J. Am. Chem. Soc.* **2006**, *128*, 15582.
[16] L. N Liu, B Li, J Ying, X. D Wu, H. F Zhao, X. G Ren, D. X Zhu, Z. M Su, *Nanotechnology* **2008**, *19*, 495709.
[17] S Jansat, K Pelzer, J García-Antón, R Raucoules, K Philippot, *Adv. Funct. Mater.* **2007**, *17*, 3339.
[18] L. M Rossi, L. F Shi, F. H Quina, Z Rosenzweig, *Langmuir* **2005**, *21*, 4277.
[19] B. P Sullivan, D. J Salmon, T. J Meyer, *Inorg. Chem.* **1978**, *17*, 3334.
[20] K Binnemans, P Lenaerts, K Driesen, C Görller-Walrand, *J. Mater. Chem.* **2004**, *14*, 191.

[21] K. R Seddon, Y. Z. T Yousif, *Met. Chem.* **1986**, *11*, 443.
[22] W Stöber, A Fink, E Bohn, *J. Colloid Interface Sci.* **1968**, *26*, 62.
[23] Y Li, B Yan, H Yang, *J. Phys. Chem. C* **2008**, *112*, 3959.
[24] P. P Yang, Z.W Quan, Z.Y Hou, C.X Li, X.J Kang, Z.Y Cheng, J Lin, *Biomaterials* **2009**, *30*, 4786.
[25] H Xia, Y. Y Zhu, D Lu, M Li, C. B Zhang, B Yang, *J. Phys. Chem. B* **2006**, *110*, 18718.
[26] P Innocenzi, H Kozuka, T Yoko, *J. Phys. Chem. B* **1997**, *101*, 2285.
[27] M. T Murtagh, M. R Shahriari, M Krihak, *Chem. Mater.* **1998**, *10*, 3862.
[28] T. J Meyer, *Pure. Appl. Chem.* **1986**, *58*, 1193.
[29] J. V Caspar, B. P Sullivan, E. M Kober, T. J Meyer, *Chem. Phys. Lett.* **1982**, *91*, 91.
[30] V. O Stern, M Volmer, *Phys Zeitschr.* **1919**, *20*, 183.
[31] B. F Lei, B Li, H. R Zhang, S. Z Lu, Z. H Zheng, W. L Li, Y Wang, *Adv. Funct. Mater.* **2006**, *16*, 1.